Journal of Ceramic Science and Technology

J. Ceram. Sci. Technol., **14** [1] 25-30 (2023)
DOI: 10.4416/JCST2022-00013
available online at: http://www.ceramic-science.com

Synthesis, Phase Evolutions, and Properties of the Perovskite $Ba_6Ca_2Ti_2Nb_3O_{19.5}$

Zh. Pan*, H. Wei, J. Xu, L. Fang, X. Kuang

MOE Key Laboratory of New Processing Technology for Nonferrous Metal and Materials; Guangxi Universities Key Laboratory of Non-ferrous Metal Oxide Electronic Functional Materials and Devices; College of Materials Science and Engineering, Guilin University of Technology, Guilin 541004, P. R. China

received December 16, 2022; received in revised form Febuary 2, 2023; accepted Febuary 2, 2023

Abstract

In the present study, $Ba_6Ca_2Ti_2Nb_{2+x}O_{17+2.5x}$ (BCTN, $x \leq 1.0$) materials were synthesized with the traditional solid-state reaction method. The phase evolution, structure, relative permittivity, and electrical conduction properties of these materials were studied. The results revealed that increasing the Nb content and improving the calcining temperature favored the formation of a pure simple cubic perovskite structure. For the end member of $Ba_6Ca_2Ti_2Nb_{2+x}O_{17+2.5x}$, i.e. $Ba_6Ca_2Ti_2Nb_3O_{19.5}$, Rietveld structural refinement disclosed that about 25 % Ca ions and all the Ba ions occupied the A site, while the remaining cations were disordered and occupied the B site. Thus, it can also be written as $(Ba_6Ca_{0.5})(Ca_{1.5}Ti_2Nb_3)O_{19.5}$. This material exhibited high permittivity up to 80 and the electrical conductivity was 1.33×10^{-4} S/cm at 800 °C which was dominated by electronic conduction.

Keywords: $Ba_6Ca_2Ti_2Nb_3O_{19.5}$, simple cubic perovskite, B-site disorder, high permittivity, alternating current impedance.

I. Introduction

Perovskite oxides, due to their diverse structural features and interesting physical and chemical properties, are important in current solid-state chemistry and physics, and have wide application [1,2]. Thanks to their high relative permittivity, which is desirable for minimization of the microwave circuit component [3,4], ABO_3-type perovskite materials have been very attractive for the electronics industry over the past 30 years. The cubic ABO_3 perovskite structure consists of a three-dimensional array of corner-sharing BO_6 octahedra, with the larger A cations in a 12-coordinate site, and arises from ordered B cation occupancy of 25 % of the octahedral sites between close-packed AO_3 layers stacked along the <111> direction of the cubic unit cell, as shown in Fig. 1. Cation site order in perovskite-derived structures is important, as it can control the physical properties such as dielectric loss [5,6], magnetoresistance [7], magnetic order [8,9], and ionic mobility [10,11]. The cation order is of particular importance for controlling microwave dielectric properties [5,12], such as the permittivity at microwave frequencies.

In 2008, Kuang *et al.* [1] reported a new six-layer perovskite-related structure $Ba_6Na_2Nb_2M_2O_{17}$ (M = P, V), which consists of cubic (c) BaO_3 layers and oxygen-deficient pseudocubic (c′) BaO_2 layers stacked in the sequence c′ccccc. In $Ba_6Na_2Nb_2M_2O_{17}$, two-dimensional slabs of the well-known 2:1 octahedral cation-ordered perovskite motif are isolated between layers of tetrahedral units formed by anion vacancy ordering: two consecutive NbO_6 octahedral layers are sandwiched by two single NaO_6 octahedral layers, which, in turn, connect with two isolated MO_4 tetrahedral layers. Both oxides are derived from the 2:1 ordered perovskite structure (e.g. $Ba_3ZnTa_2O_9$) [13] by the ordered removal of O atoms in every sixth BaO_3 layer. Both materials exhibit a relative permittivity of ~ 20 – 23.

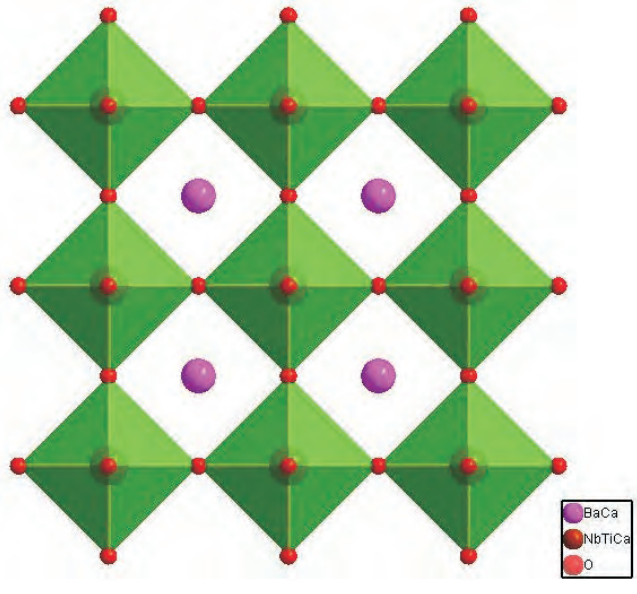

Fig. 1: The crystal structure of a typical simple cubic perovskite.

* Corresponding author: pzw12212287@163.com

In this work, we originally intended to replace the Na and P/V cations with Ca and Ti, respectively, to prepare the $Ba_6Ca_2Ti_2Nb_2O_{17}$ material with the hexagonal perovskite structure that is iso-structural with $Ba_6Na_2Nb_2M_2O_{17}$. However, the secondary cubic perovskite phase in the products could not be avoided, and increasing the Nb content would ultimately yield pure simple cubic perovskite $Ba_6Ca_2Ti_2Nb_3O_{19.5}$ as a product. This novel simple cubic perovskite material ceramicshowed high permittivity ($\varepsilon_r \sim 80$) and impedance data revealed the dominating electronic conduction, without ionic conduction being observed.

II. Experimental procedure

$Ba_6Ca_2Ti_2Nb_{2+x}O_{17+2.5x}$ (BCTN) materials were prepared based on a routine solid-state reaction, using high-purity $BaCO_3$ (99.99 %, Damao Chemical Reagent Factory), $CaCO_3$ (99.99 %; Aladdin), TiO_2 (99.99 %; Aladdin), Nb_2O_5 (99.99 %, Aladdin) as starting materials, which were dried at 400 °C for 3 hours before they were weighed. The starting materials were weighed stoichiometrically, mixed in ethanol with an agate mortar, dried at room temperature and precalcined at 1 200 °C for 12 hours in an alumina crucible with heating and cooling rates of 5 K/min. The pre-calcination process was employed to decompose the carbonate $CaCO_3$ and $BaCO_3$ into CaO, BaO, CO_2 and improve homogeneity of the mixture, which would be beneficial to the formation of pure phase product in the final sintering. The precalcined powder was then mixed with 5 % polyvinyl alcohol (PVA) solution as an organic binder and pressed into pellets under 140 MPa pressure. The pellets were buried in sacrificial powders of the same composition in aluminum crucibles covered with lids and heated at 600 °C for 100 min to remove the PVA, and then fired at 1 400 °C – 1 600 °C for 12 – 24 hours with heating rates of 5 K/min and cooling rates 0.5 K/min. The densities of the pellets were calculated by using the geometric size (diameter and thickness) and the mass of the pellets.

The phase compositions were checked by means of the powder X-ray diffraction (XRD) technique, which was performed on a D8 ADVANCE powder diffractometer with CuKα radiation. The XRD data were collected over a 2θ range of 10 – 80°. The powder XRD data was analyzed with Rietveld refinement using Topas Academic software. The microstructure of the pellets was examined using a Quanata 400F scanning electron microscope (SEM). Prior to the SEM experiment, gold was sprayed onto the surface to form a thin conducting layer.

AC impedance spectroscopy measurement was carried out on a Solartron 1260A impedance/gain-phase analyzer with the frequency range from 10^7 Hz to 10^{-1} Hz over a temperature range from room temperature to 800 °C. For these measurements, the pellets were coated with gold paste and fired at 550 °C for 90 min to remove the organic components in order to form electrodes. In order to obtain accurate permittivity of the material itself, the blank contribution arising from the sample holder and connection cables, measured on an open circuit without a pellet, was subtracted from the measured capacitance of the pellets. The microwave dielectric properties were measured with the Hakki-Coleman dielectric resonator method [3] with the TE_{011} mode using an Agilent N5230A network analyzer.

III. Results and Discussion

(1) Phase evolution of $Ba_6Ca_2Ti_2Nb_{2+x}O_{17+2.5x}$

As reported in Kuang *et.al.*'s previous work, hexagonal perovskite $Ba_6Na_2Nb_2M_2O_{17}$ (M = P, V) could be obtained with a traditional solid-state reaction method. Herein, we originally intended to completely replace the Na and M in $Ba_6Na_2Nb_2M_2O_{17}$ with Ca and Ti, respectively, to prepare the hexagonal perovskite $Ba_6Ca_2Ti_2Nb_2O_{17}$. However, mixed hexagonal and cubic perovskite phases were always there in the products, no single phase could be obtained, and changing the preparation conditions, such as increasing the temperature or prolonging the dwell time, did not work. An exemplary XRD pattern for the product of $Ba_6Ca_2Ti_2Nb_2O_{17}$ prepared at 1 500 °C for 12 hours can be seen in Fig. 2.

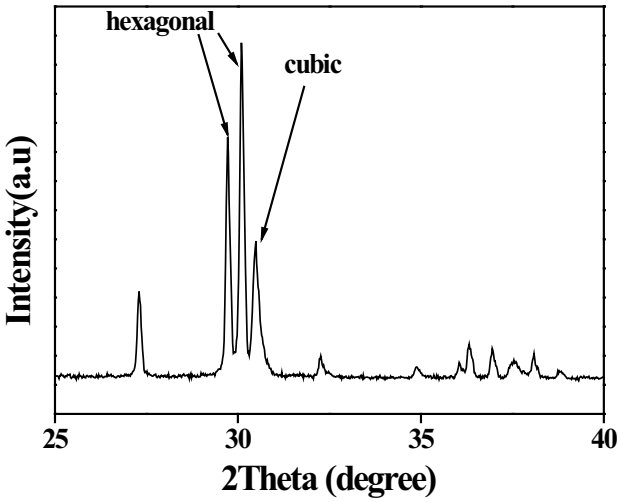

Fig. 2: XRD pattern of $Ba_6Ca_2Ti_2Nb_2O_{17}$ fired at 1 500 °C for 12 h.

Interestingly, based on the analysis of quantities of experiments, we found that increasing the Nb content would unexpectedly increase the cubic phase proportion in the products, and even a single cubic phase product could be yielded for the composition $Ba_6Ca_2Ti_2Nb_3O_{19.5}$, as shown in Fig. 3a. To investigate the exact cation distribution in the unit cell of $Ba_6Ca_2Ti_2Nb_3O_{19.5}$, Rietveld structural refinements[14] against the XRD data were carried out using the simple cubic perovskite-type $BaTiO_3$ (space group of $Pm\bar{3}m$) as a structural model, with one A site (1a for Ba), one B site (1b for Ti), and one C site (3c for oxygen). The refinement confirmed that besides all the Ba ions, 1/4 of the Ca ions in $Ba_6Ca_2Ti_2Nb_3O_{19.5}$ are also located in the A site, while the remaining Ca ions and all the Ti and Nb ions are randomly distributed in the B site. The Rietveld fitting plots of the XRD data for $Ba_6Ca_2Ti_2Nb_3O_{19.5}$ are shown in Fig. 3b. The final refined structural parameters of $Ba_6Ca_2Ti_2Nb_3O_{19.5}$ are listed in Table 1.

Table 1: The final refined structural parameters for $Ba_6Ca_2Ti_2Nb_3O_{19.5}$.

Atoms	Site	*x*	*y*	*z*	Occupancy	B_{iso}(Å^2)
Ba	1a	0	0	0	0.923(1)	1.61(4)
Ca1	1a	0	0	0	0.077(1)	1.61(4)
Ca_2	1b	0.5	0.5	0.5	0.231(1)	1.15(3)
Ti	1b	0.5	0.5	0.5	0.307(2)	1.15(3)
Nb	1b	0.5	05	0.5	0.462(1)	1.15(3)
O	3c	0	0.5	0.5	1	2.36(2)

a = 4.13177(3), Space group: $Pm\bar{3}m$, R_{wp}=6.69 %, R_b=2.69 %, R_p= 4.47 %.

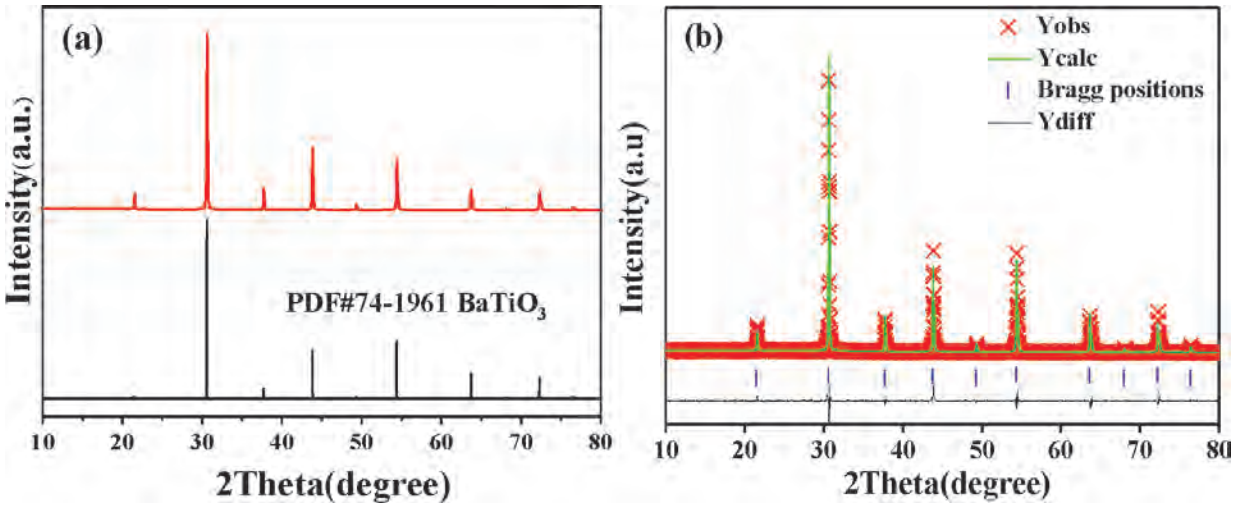

Fig. 3: (a) XRD data and (b) corresponding Rietveld fitting plots of $Ba_6Ca_2Ti_2Nb_3O_{19.5}$.

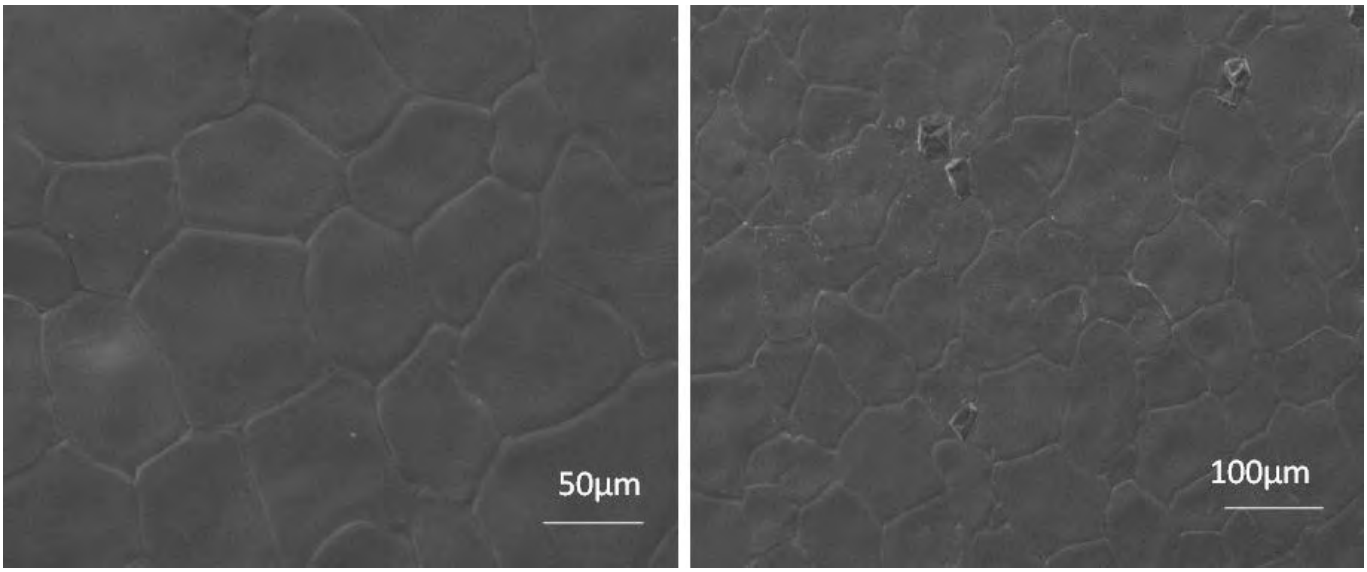

Fig. 4: SEM images of surface morphologies of the $Ba_6Ca_2Ti_2Nb_3O_{19.5}$ pellets.

The microstructure of the $Ba_6Ca_2Ti_2Nb_3O_{19.5}$ pellet fired at 1 500 °C for 12 hours was then examined by means of SEM, as shown in Fig. 4. The images showed a dense microstructure free of pores, which is consistent with its relative density of ~ 93 %, which was calculated based on the geometric size (diameter and thickness) and the mass of the pellet. The grains sizes are mainly in the range of 50 – 100 μm with well-defined grain boundaries.

AC impedance spectroscopies [15] were then recorded on the dense pellet of the $Ba_6Ca_2Ti_2Nb_3O_{19.5}$ sample. The impedance showed two separated arcs within the whole measured temperature range, as can be seen from Fig. 5

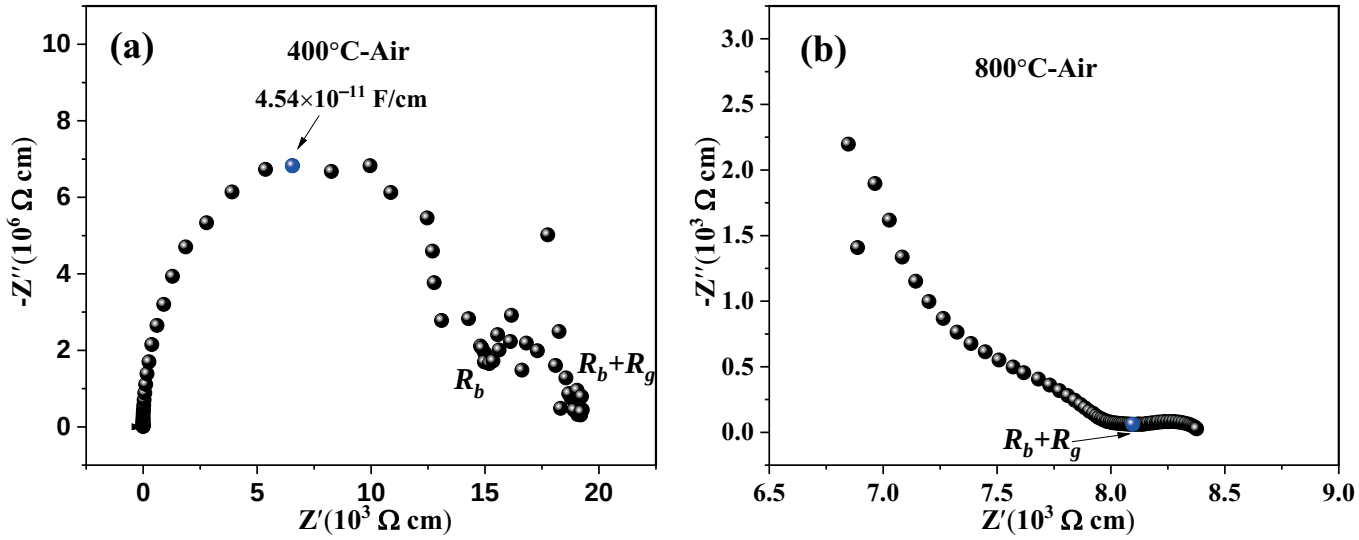

Fig. 5: Impedance plots of $Ba_6Ca_2Ti_2Nb_3O_{19.5}$ measured at 400 and 800 °C.

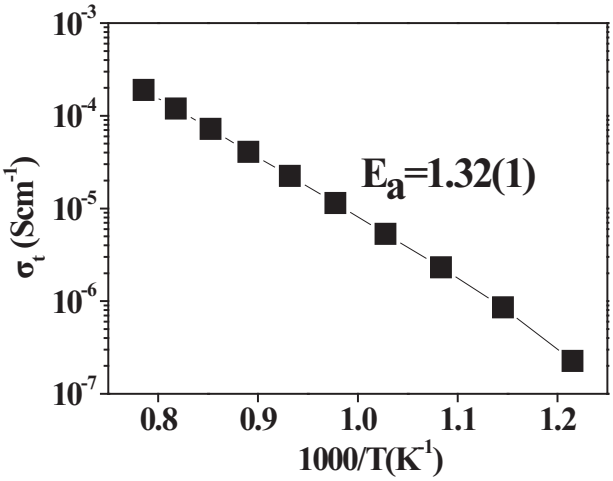

Fig. 6: Arrhenius plots of bulk conductivity for $Ba_6Ca_2Ti_2Nb_3O_{19.5}$.

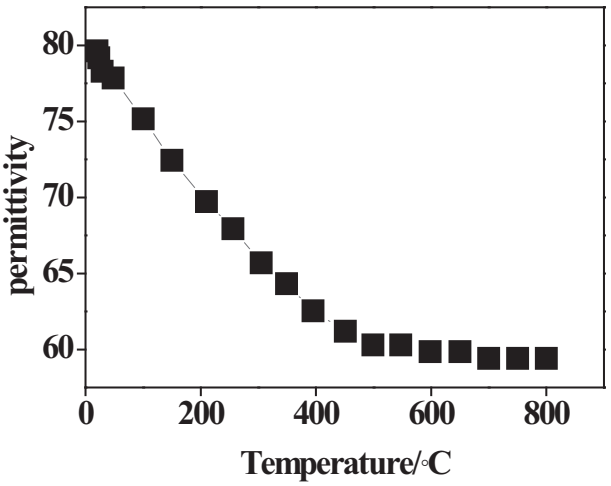

Fig. 7: Permittivity of $Ba_6Ca_2Ti_2Nb_3O_{19.5}$ pellets collected from 25 °C – 800 °C.

for the impedance plots recorded at 400 °C and 800 °C. The arcs in the high- and low-frequency range corresponded to the grain and grain boundary response, respectively. No electrode response was observed, which excluded the ionic conduction in this material. The total resistivity of the $Ba_6Ca_2Ti_2Nb_3O_{19.5}$ pellet was simply estimated as the intercept of the semicircular arc at low frequency. The Arrhenius plot of total conductivities for the $Ba_6Ca_2Ti_2Nb_3O_{19.5}$ pellet is shown in Fig. 6. The conductivity of $Ba_6Ca_2Ti_2Nb_3O_{19.5}$ ceramic varied within 2.53×10^{-7}-1.33×10^{-4} S/cm in 300 – 800 °C.

The dielectric constants (ε_r) obtained from the impedance spectroscopies showed a decrease from ε_r ~ 80 at room temperature to ε_r ~ 60 at 800 °C (Fig. 7). The temperature coefficient of permittivity ranged in 10^{-3} – 10^{-5} from room temperature to 400 °C, as shown in Fig. 8.

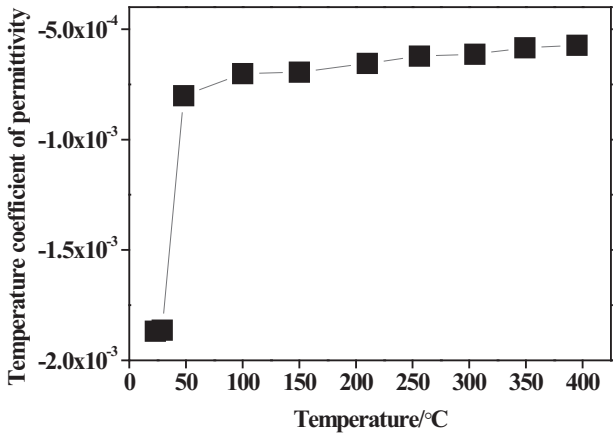

Fig. 8: The temperature coefficient of permittivity of $Ba_6Ca_2Ti_2Nb_3O_{19.5}$.

IV. Conclusions

The $Ba_6Ca_2Ti_2Nb_{2+z}O_{17+\delta}$ (BCTN) materials were synthesized with a traditional solid-state reaction method. The phases, structures, and electrical properties were studied. The results revealed that the Nb content increase fa-

vored the formation of pure simple cubic-perovskite-structured $Ba_6Ca_2Ti_2Nb_3O_{19.5}$. The Rietveld structural refinement showed that about 25 % of Ca ions and all the Ba ions occupied the A site, while the remaining cations were disordered and occupied the B site. The electrical conductivity of this material was 2.52×10^{-7}-1.23×10^{-4} S/cm within the temperature range of 300 – 800 °C and dominated by electronic conduction. The dielectric constants decreased from 80 at room temperature to ~ 60 at 800 °C.

Acknowledgments

The National Science Foundation of China (Nos. 21965008, 21361008), Guangdong Natural Science Foundation (S2011010001310), and Guangxi Key Laboratory for Advanced Materials and New Preparation Technology (No. 12AA-11) are acknowledged for their financial support. We thank Xiaolan Yu (Sun Yat-Sen University) for assistance with XRD measurements.

References

1 Kuang, X.-J., Price, T., Iddles, D.M., Rosseinsky, M.J.: Isolation of two-dimensional 2:1 cation-ordered perovskite units by anion vacancy ordering in $Ba_6Na_2Nb_2P_2O_{17}$, *Inorg. Chem.*, **47**, [19], 8444 – 50, (2008).

2 Kaletsch, A., Bezold, A., Pfaff, E.M., Broeckmann, C.: Effect of copper oxide content in AgCuO braze alloy on microstructure and mechanical properties of reactive-air-brazed $Ba_{0.5}Sr_{0.5}Co_{0.8}Fe_{0.2}O_3$(BSCF), *J. Ceram. Sci. Technol.,* **03**, [02], 95 – 104, (2012).

3 Jancar, B., Suvorov, D., Valant, M., Drazic, G.: Characterization of $CaTiO_3$-$NdAlO_3$ dielectric ceramics, *J. Eur. Ceram. Soc.,* **23**, [9], 1391 – 400, (2003).

4 Kuang, X.-J., Allix, M.M.B., Claridge, J.B., Niu, H.-J., Rosseinsky, M.J, Ibberson, R.M., Iddles, D.M.: Crystal structure, microwave dielectric properties and AC conductivity of B-cation deficient hexagonal perovskites $La_5M_xTi_{4-x}O_{15}$ (x = 0.5, 1; M = Zn, Mg, Ga, Al), *J. Mater. Chem.,* **16**, [11], 1038, (2006).

5 Davies, P.K.: Cation ordering in complex oxides, *Curr. Opin. Solid State Mater. Sci.,* **4**, 467 – 71, (1999).

6 Liu, Y., Huang, X.: High permittivity and dielectric response of $CaCu_3Ti_{3.9}(Y_{0.5}Nb_{0.5})_{0.1}O_{12}$ Ceramics, *J. Ceram. Sci. Technol*., **08**, [2], 243 – 48, (2017).

7 Huang, Y.-H., Karppinen, M., Yamauchi, H., Goodenough, J.B.: Systematic studies on effects of cationic ordering on structural and magnetic properties in Sr_2FeMoO_6, *Phys Rev. B.,* **73**, [10], 104408 – 1-5, (2006).

8 Rodgers, J.A., Battle, P.D., Dupre, N., Grey, C.P., Sloan, J.: Cation and spin ordering in the n =1 ruddlesden-popper phase $La_2Sr_2LiRuO_8$, *Chem. Mater.,* **16**, [22], 4257 – 66, (2004).

9 Millange, F., Caignaert, V., Domenges, C., Raveau, B.: Order-disorder phenomena in new $LaBaMn_2O_{6-x}$ CMR perovskites crystal and magnetic structure, *Chem. Mater.,* **10**, [7], 1974 – 83, (1998).

10 Kim, S.W.G., Jacobson, A.J.: Oxygen exchange kinetics of epitaxial $PrBaCo_2O_5$ thin films, *Appl. Phys. Lett.,* **88**, [24103], 1 – 3, (2006).

11 Harada, Y.H., Hirakoso, Y.J., Kawai, H., Kuwano, J.: Order-disorder of the A-site ions and lithium ion conductivity in the perovskite solid solution $La_{0.67-x}Li_{3x}TiO_3$ (x= 0.11), *Solid State Ionics,* **121**, 245 – 51, (1999).

12 Thirumal, M., Davies, P.K.: $Ba_8ZnTa_6O_{24}$: A new high q dielectric perovskite, *J. Am. Ceram. Soc,* **88**, [8], 2126 – 28, (2005).

13 Surendran, K.P., Sebastian, M.T.: Low loss dielectrics in $Ba[(Mg_{1/3}Ta_{2/3})_{1-x}Ti_x]O_3$ and $Ba[(Mg_{1-x}Zn_x)_{1/3}Ta_{2/3}]O_3$ systems, *J. Mater. Res.,* **20**, [11], 2919 – 26, (2005).

14 Rietveld, H.M.: A profile refinement method for nuclear and magnetic structures, *J. Appl. Cryst.,* **2**, [65], 65 – 71, (1969).

15 Irvine, T.S., Sinclair, D.C., West, A.R.: Electroceramics characterization by impedance spectroscopy, *Adv. Mater.,* **2**, [3], 132 – 38, (1990).